Carbon Capture Science & Technology 11 (2024) 100188

Contents lists available at ScienceDirect

Carbon Capture Science & Technology

journal homepage: www.elsevier.com/locate/ccst

Full Length Article

Estimating the line packing time for pipelines transporting carbon dioxide

Sergey B. Martynov*, Richard T.J. Porter, Haroun Mahgerefteh

Department of Chemical Engineering, University College London, Torrington Place, London WC1E 7JE, United Kingdom

A R T I C L E I N F O

Keywords:
CO_2 transport
Pipeline
Line pack
Unpacking
Transients
Operational flexibility

A B S T R A C T

During the operation of pressurised pipelines transporting compressible fluids, line packing is employed as an effective method that uses the pipeline itself as a buffer storage, compensating for fluctuations in the fluid supply or demand. While in large-capacity natural gas transmission systems, reaching maximum operating pressures during line packing is usually not of practical concern, in small capacity pipelines transporting low-compressibility fluids, such as liquid or dense-phase CO_2, line packing can occur quickly, and therefore, estimating the line packing times becomes important to ensure avoiding exceeding the pipeline maximum allowable operating pressure. In this study, a correlation for estimating the line packing time is derived from the transient mass balance in the pipeline. The proposed correlation accounts for the pipeline overall dimensions, operating pressure and temperature, and the fluid properties, namely density and the expansion coefficient. The correlation is also adopted for the calculation of pipeline unpacking times caused by unbalanced discharge from a pipeline. A verification study on line packing in a dense-phase CO_2 pipeline shows that within the ranges tested, the proposed correlation estimates conservatively the line packing times with ca. 15 % deviation from the results of simulations obtained using a rigorous transient pipeline flow model. The proposed correlation is also verified against predictions obtained using a parabolic flow model and is recommended for estimating line packing times for both dense-phase and gas-phase CO_2 at pressures and temperatures in the ranges 2 - 12 MPa and 280 – 330 K, respectively. The limitations of the proposed line packing time correlation are discussed.

1. Introduction

During the operation of pipelines transporting compressible fluids, line packing is a method that uses the pipeline itself as a buffer storage, compensating for fluctuations in the fluid supply or demand. The method is widely used in natural gas transmission and distribution pipelines (Pambour et al., 2017; Shashi Menon, 2005) and can become useful to ensure flexible and safe operation of large CO_2 pipeline transportation systems (Mac Dowell and Staffell, 2016; Spitz et al., 2018) which are emerging as an essential element of the Carbon Capture, Utilisation and Storage (CCUS) technologies designed to mitigate the global warming caused by anthropogenic CO_2 emissions into the atmosphere (Doctor et al., 2005; Ejeh et al., 2022; ZEP, 2020). However, in contrast with the natural gas transportation, where the line packing problem mainly concerns scheduling the gas supply under fluctuating/ uncertain demand, in CO_2 pipeline transportation, due to low compressibility of dense-phase CO_2, line packing may result in a rapid increase of fluid pressure up to the Maximum Allowable Operating Pressure (MAOP) corresponding to tensile strength of a pipeline (Oosterkamp and Ramsen, 2008; Rackley, 2010). Therefore, estimating line packing times becomes critically important for adopting suitable control strategies for safe operation of CO_2 pipelines (Peplinski, 2012; White Rose, 2015).

Computational flow models are commonly used to predict the linepack amount and transient line packing scenarios in natural gas pipelines (Abbaspour et al., 2007; Ahmadian Behrooz and Boozarjomehry, 2017; Chertkov et al., 2015; Pambour et al., 2016; Ríos-Mercado and Borraz-Sánchez, 2015). These models are particularly useful for analysis of line packing in complex scenarios of operation of long pipelines and pipeline networks. However, in conceptual engineering design, simpler algebraic correlation for the linepack capacity and line packing time are needed.

Recently, Aghajani et al. (2017) applied a transient flow model to simulate scenarios of line packing in dense-phase CO_2 in pipelines, predicting the line packing times for a range of pipeline design and operational parameters (pipeline outer diameter from 457 to 914 mm, pipe wall thickness from 8 to 20 mm, pipe length from 50 to 150 km, mass flow rate from 35 to 150 kg/s, pipeline operating pressure from 8.7 to 11 MPa, MAOP from 11.3 to 15.6 MPa). Although the authors have explained individual effects of some of these factors (pipeline diameter, length, inlet flow and MAOP) and applied a neural network modelling

Abbreviations: AAD, Absolute Average Deviation; CCUS, Carbon Capture, Utilization and Storage; MAOP, Maximum Allowable Operating Pressure.

* Corresponding author.
E-mail address: s.martynov@ucl.ac.uk (S.B. Martynov).

https://doi.org/10.1016/j.ccst.2023.100188
Received 15 October 2023; Received in revised form 8 December 2023; Accepted 24 December 2023

approach to simulate their integral impact, so far no generalized close form approximation for line packing time has been constructed.

Accounting for line packing is also important for control of operability issues that may arise due to flashing of liquid CO_2 and transition to two-phase flow when pressure is reduced to below the bubble line pressure in scenarios of unbalanced discharge of fluid from the pipe – the phenomenon commonly known as unpacking (also called depacking or drafting) (Daud, 2018; Oosterkamp and Ramsen, 2008; White Rose, 2015). In this case, implementing suitable flow assurance control measures requires estimating the pipeline unpacking time, which however has received only little attention in literature.

To this end, the present study is aimed at deriving an algebraic correlation for line packing time based on a physical pipe flow model and applying it for calculating line packing times for pipelines transporting CO_2. In Section 2, the two most commonly used transient pipe flow models are introduced, providing the basis for linepack analysis in this study. In Section 3, correlations for line packing and unpacking times are derived. Section 4 presents the results of verification of the line packing time correlation against the transient model simulations for high-pressure CO_2 pipelines, and parametric studies of the impacts of operating pressure and temperature on line packing times. Section 5 summarises the key findings and conclusions from the study.

2. Theory and methods

2.1. Hyperbolic flow model

The governing equations describing transient one-dimensional single-phase flow in a horizontal pipe include the mass, momentum and energy equations that can be written in the following form (Aursand et al., 2013):

$$\frac{\partial \rho}{\partial t} + \frac{\partial (\rho u)}{\partial x} = 0 \tag{1}$$

$$\frac{\partial (\rho u)}{\partial t} + \frac{\partial \left(\rho u^2\right)}{\partial x} + \frac{\partial p}{\partial x} = -f \frac{\rho\, u\, |u|}{2D} \tag{2}$$

$$\frac{\partial E}{\partial t} + \frac{\partial [u(E + p\,)]}{\partial x} = \frac{4 q_w}{D} - f \frac{\rho u^3}{2D} \tag{3}$$

where ρ, u and p are respectively the fluid density, the flow velocity and the fluid pressure, respectively. t is time, x is the spatial coordinate along the pipe, D, f and q_w are respectively the pipe inner diameter, the Darcy friction factor and the heat flux at the pipe wall, and E is the total energy density of the fluid, defined as:

$$E = \rho \left(e + \frac{1}{2} u^2 \right) \tag{4}$$

Here e is the internal energy of the fluid, which can be calculated as a function of the fluid temperature, pressure and composition.

In the present study, the friction factor is calculated using the Colebrook-White equation (Coulson and Richardson, 1999):

$$f = 0.25 \left[\lg \left(\frac{\epsilon}{3.7\, D} + \frac{5.74}{Re^{0.9}} \right) \right]^{-2} \tag{5}$$

where ϵ and $Re = \frac{\rho u D}{\mu}$ are respectively the wall roughness and the flow Reynolds number, while μ is the coefficient of dynamic viscosity of the fluid.

In Eq. (4), the heat flux is defined by Newton's law:

$$q_w = h \left(T_{amb} - T \right) \tag{6}$$

where T and T_{amb} are respectively the temperatures of the fluid inside the pipe and its surrounding, and h is the overall heat transfer coefficient at the pipe wall.

The above equations can be solved numerically subject to initial and boundary conditions and suitable physical properties models.

For line packing scenarios involving sub-sonic flows, the boundary conditions can be specified by prescribing two flow variables at the pipe inlet (e.g., the inlet mass flowrate and pressure) and one variable at the pipe exit (e.g., the outlet flowrate). The initial conditions can be obtained by integrating the steady-state version of the above equations given the mass flowrate and the inlet pressure and temperature.

It can be noted that for steady-state incompressible flow, integration of the momentum equation gives linear pressure drop in the pipe, while integration of the energy equation over the pipe length results in the following initial temperature distribution along the pipe (Martynov et al., 2015):

$$T_o(x) = T_{amb} + \left(T_{in} - T_{amb} \right) \cdot \exp\left(-\frac{4\, h}{\rho u\, c_p} \frac{x}{D} \right) \tag{7}$$

where T_{in} is the temperature of fluid at the pipe inlet, and c_p is the specific heat capacity of the fluid, which can be evaluated at the average pressure and temperature of fluid in the pipe segment.

2.2. Parabolic flow model

The parabolic flow model is a reduced form of the hyperbolic model presented in Section 2.1, obtained by retaining the continuity and momentum conservation equations, with the inertia terms neglected in the momentum equation as an approximation, and discarding the energy balance equation assuming isentropic or isothermal flow (Osiadacz, 1984):

$$\frac{\partial \rho}{\partial t} + \frac{\partial (\rho u)}{\partial x} = 0 \tag{8}$$

$$\frac{\partial p}{\partial x} = -f \frac{\rho\, u\, |u|}{2D} \tag{9}$$

Eqs. (8) and (9) are widely used for simulation of slow transients in pipes and pipeline networks, e.g., for optimisation of line packing in natural gas distribution networks (Ahmadian Behrooz and Boozarjomehry, 2017; Chertkov et al., 2015; Pambour et al., 2017).

Solving the above equations requires knowledge of initial conditions, the feed flow rate and pressure boundary conditions as well as correlations for the calculation of the relevant physical properties of the transported fluid. In the present study, the boundary conditions for the line packing problem are specified by prescribing the fluid mass flowrates at the pipeline inlet and outlet. At time $t = 0$ the mass flowrate is set constant and the pressure variation in the pipe is obtained by integrating the momentum Eq. (9) assuming constant density (incompressible flow).

2.3. Numerical solution

To perform the numerical solution of the parabolic equations of Section 2.2, they were converted to a non-linear "diffusion" type Partial Differential Equation (PDE) in pressure (see Appendix for the derivation):

$$\frac{1}{c_z^2} \sqrt{\frac{2\, f}{\rho\, D} \left| \frac{\partial p}{\partial x} \right|} \frac{\partial p}{\partial t} - \frac{1}{\rho c_z^2} \left(\frac{\partial p}{\partial x} \right)^2 - \frac{\partial^2 p}{\partial x^2} = 0 \tag{10}$$

where c_z is the process-specific speed of sound, with the index "z" referring to the thermodynamic variable that is kept constant (e.g., temperature or entropy).

In the present study the boundary conditions for Eq. (10) are specified based on the mass flowrates prescribed at the inlet and outlet of the pipe:

$$x = 0: \quad \frac{\partial p_{in}}{\partial x} = -f \frac{G_{in}^2}{2 \rho_{in} A^2 D} \tag{11}$$

$$x = L:\ \frac{\partial p_{out}}{\partial x} = -f\frac{G_{in}^2}{2\rho_{in}A^2 D} \tag{12}$$

where indices "*in*" and "*out*" refer to the inlet and outlet locations, $G = \rho\ u\ A$ is the mass flowrate, and $A = \pi\ D^2\ /\ 4$ is the pipe cross sectional area.

The initial pressure distribution in the pipe is calculated using the integral form of Eq. (9):

$$t = 0:\ p_o(x) = p_{in,\ o} - f\frac{G_o^2}{2\rho_o A^2}\frac{x}{D} \tag{13}$$

where index "o" denotes the initial state at $t = 0$.

The numerical solution of Eqs. (10–13) is obtained using the second order accurate in space method of lines (Skeel and Berzins, 1990) which discretises the spatial domain into N_x elements and transforms the PDE Eq. (10) into a set of Ordinary Differential Equations (ODEs). The ODEs are then solved using a variable time stepping method in the PDEPE function in MatLab (MathWorks, 2023). A purpose written MatLab script for solving Eqs. (10–13) is made available in Supporting Information. The relevant physical properties of CO_2 fluid, including the density, the speed of sound and dynamic viscosity that appear in the model equations, are calculated using REFPROP package implementing the Span and Wagner equation of state (Lemmon et al., 2018; Span and Wagner, 1996).

3. Line packing and unpacking times

3.1. Line packing time

For engineering calculations, of particular interest are simple algebraic correlations predicting the linepack amount and the line packing time. These two parameters are commonly defined for a scenario where a pipeline, initially operating in steady-state, is isolated at the outlet while the inlet flowrate is kept constant, as schematically presented in Fig. 1. In a more general scenario, the linepack is caused by imbalance of the inlet and outlet flow rates, e.g., when the outlet flow rate, G_{out} is less than the inlet flow rate G_{in}. The line pack amount, ΔM_{LP}, is then defined as the extra amount of fluid accumulated in the pipeline on the top of its nominal operating capacity. The line packing time, t_{LP}, is the duration that it takes for the pipeline pressure to rise from the initial pressure, p_o, to the line packing pressure, p_{LP}. The history of the pressure variation can be predicted, e.g., by solving the transient flow models of Section 2.

The two parameters are linked to each other in the integral form of the pipeline mass conservation equation, which is in turn obtained by integrating the continuity Eq. (1) over time and length of the pipe:

$$\int_0^{t_{LP}}\int_0^{L}\frac{\partial\rho}{\partial t}dx\,dt \approx -\int_0^{t_{LP}}\int_0^{L}\frac{\partial(\rho u)}{\partial x}dx\,dt \tag{14}$$

Approximating the integrals in this equation using the mean value theorem gives:

$$L\int_0^{t_{LP}}\frac{\partial\bar{\rho}}{\partial t}dt \approx -t_{LP}\int_0^{L}\frac{\partial(\widetilde{\rho u})}{\partial x}dx \tag{15}$$

where $\bar{\rho} = \int_0^L \rho\ dx$ is the fluid density averaged over the pipe length, and $(\widetilde{\rho u}) = \int_0^{t_{LP}} \rho u\ dt$ is the mass flux averaged over the time t_{LP}.

Introducing the notation $\widetilde{\rho u}(x = 0, t) = \rho_{in}u_{in}$ and $\widetilde{\rho u}(x = L, t) = \rho_{out}u_{out}$, and subsequently rearranging for t_{LP} gives:

$$t_{LP}\ \approx\ \frac{V\ (\bar{\rho}_{LP} - \bar{\rho}_o)}{\Delta G} \equiv \frac{\Delta M_{LP}}{\Delta G} \tag{16}$$

where $\Delta G = (\rho_{in}u_{in} - \rho_{out}u_{out})A = G_{in} - G_{out}$ is the mass flowrate imbalance between the inlet and outlet of the pipeline, A and V are the pipeline cross-sectional area and volume, and indexes "o" and "LP" refer to conditions in the pipe at the initial moment $t = 0$ and the final time t_{LP}.

Using the process-specific expansion coefficient $\kappa_z = \frac{\rho}{p}\left(\frac{\partial p}{\partial\rho}\right)_z \equiv \frac{\rho\ c_z^2}{p}$, the density variation in Eq. (16) can be approximated to the first order as:

$$(\bar{\rho}_{LP} - \bar{\rho}_o) \approx \frac{\bar{\rho}_o}{\kappa_{z,o}}\cdot\frac{(\bar{p}_{LP} - \bar{p}_o)}{\bar{p}_o} \tag{17}$$

which upon substitution into Eq. (16) gives:

$$t_{LP}\ \approx\ \frac{\bar{\rho}_o}{\kappa_{z,o}}\cdot\frac{V}{\Delta G}\cdot\frac{(\bar{p}_{LP} - \bar{p}_o)}{\bar{p}_o} \tag{18}$$

Eq. (13) provides a correlation for estimating the line packing time as a function of the pipe volume, inlet mass flowrate and initial and final operating pressures, and also the expansion coefficient $\kappa_{z,o}$ specific to the line packing process.

3.2. Unpacking time

Although the present study is focused on the line packing phenomenon, the analysis presented in Section 3.1 can be applied to unpacking operation where discharge of fluid from a pipeline is accompanied by pressure drop to a minimum threshold, p_{min}, prescribed according to the hydraulic operation and flow assurance criteria [see, e.g., (Daud, 2018; Oosterkamp and Ramsen, 2008; Rose, 2015)]. The unpacking may happen, e.g., in a scenario of unbalanced discharge of fluid during the inlet compressor trip. In this case, Eq. (18) is rewritten in the following form to give an estimate for the unpacking time:

$$t_{UP}\ \approx\ \frac{\bar{\rho}_o}{\kappa_{z,o}}\cdot\frac{V}{\Delta G}\cdot\frac{(\bar{p}_o - p_{\min})}{\bar{p}_o} \tag{19}$$

where $\Delta G = G_{out} - G_{in}$ is the cumulative discharge mass flowrate from the pipe.

4. Results and discussion

4.1. Verification of the line packing time correlation

In this section, Eq. (18) is applied to predict line packing times in dense-phase CO_2 transportation pipelines for a scenario studied by

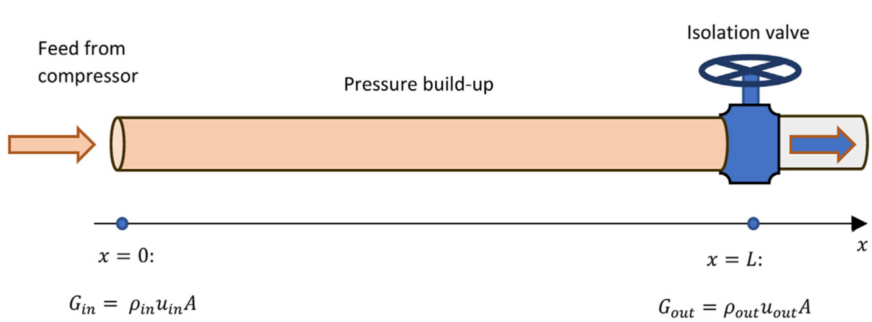

Fig. 1. Schematic of a pipeline undergoing line packing due to imbalanced inlet and outlet flowrates.

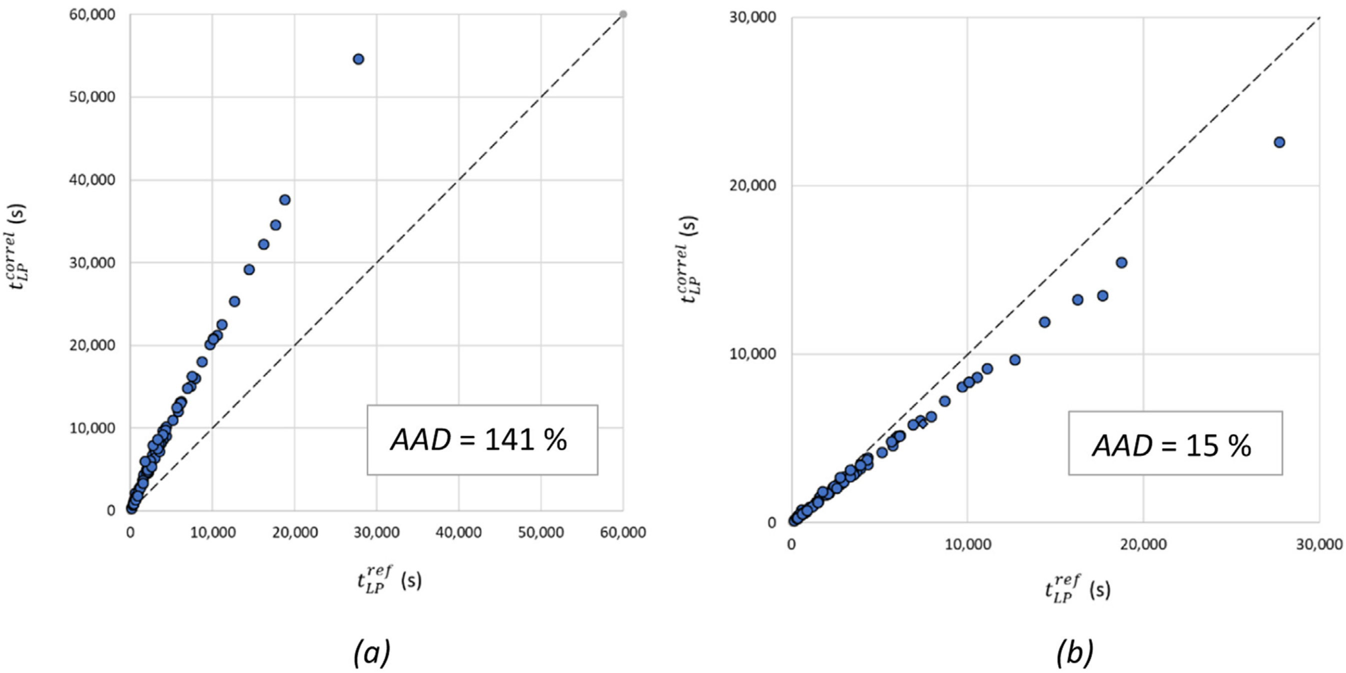

Fig. 2. Parity plots comparing the line packing times t_{LP}^{correl} estimated using Eq. (18) in the present study, assuming isothermal (a) and isentropic (b) line packing, and t_{LP}^{ref} predicted by Aghajani et al. (2017).

Aghajani et al. (2017). The modelled scenario involved closure of an isolation valve at the pipe outlet as shown in Fig. 1. In the above study, the authors constructed 81 test cases to cover practically relevant ranges of pipeline outer diameters (457 to 914 mm), lengths (50 to 150 km), wall thicknesses (8 to 20 mm) and also operating pipeline inlet pressures (8.7 to 11 MPa) and flowrates (35 to 150 kg/s). In addition to these parameters, the inputs to the model also included the pipeline final operating pressure $\bar{p}_{LP}$ that was set to the pipeline MAOP.

When applying Eq. (18), the expansion coefficient $\kappa_{z,o}$ was calculated for scenarios of isothermal and isentropic compression. It can be noted that for the isothermal case, Eq. (16) can be used directly, with the density $\bar{\rho}_{LP}$ calculated at $\bar{T}_o$ and $\bar{p}_{LP}$. The initial average pressure in the pipe, $\bar{p}_o$, was obtained as the mean average of the pipe inlet pressure and the outlet pressure calculated using Eq. (13). In Eq. (5), the wall roughness $\epsilon = 0.0457$ mm was used. The fluid initial pipeline average temperature $\bar{T}_o$ was calculated using Eq. (7), assuming the overall heat transfer coefficient $h = 2.5\text{W m}^{-2}$, the inlet temperature of 303 K and the ambient temperature of 278 K. Given that physical properties in Eqs. (7) and (13) depend on $\bar{T}_o$ and $\bar{p}_o$, which are not known *a priori*, several iterations were performed to resolve the initial pressure and temperature profiles in the pipe and the corresponding average properties, including density $\bar{\rho}_o$ and the expansion coefficient $\bar{\kappa}_{z,o}$ calculated using the reference equation of state in REFPROP (Lemmon et al., 2018).

The conditions for the tests along with the results of calculations are provided in the Supporting Information.

Fig. 2 provides the parity plots showing the deviations of predictions of the line packing time by Eq. (18), t_{LP}^{correl}, from the reference data t_{LP}^{ref} obtained by Aghajani et al. (2017). The results in subplot (a) were obtained using Eq. (18) with the isothermal expansion coefficient, while in subplot (b) the isentropic expansion was assumed. The figures also report the Absolute Average Deviations (%*AAD*) of t_{LP}^{correl} from t_{LP}^{ref} for the entire data set ($N = 81$ points):

$$AAD = \sum_{i=1}^{N=81} \left| 1 - \frac{t_{LP,i}}{t_{LP,i}^{ref}} \right| \times 100\% \tag{20}$$

Comparison of the results in Fig. 2a and b shows that using the isentropic expansion coefficient in Eq. (18) (Fig. 2b) gives much better agreement with the reference data (slightly underestimating the line packing times, with AAD = 15 %) than assuming the isothermal line packing (Fig. 2a, AAD = 141 %). The relatively large deviations in the isothermal case can be attributed to the fact that for the pressure and temperature conditions studied, the isothermal expansion coefficient of CO_2, κ_t, is typically several times smaller than its isentropic analogue, κ_s, that according to Eq. (17), translates in much larger density changes of the fluid upon the line packing. On the other hand, the relatively small scatter of the data in Fig. 2b (AAD = 15 %) shows that under the isentropic assumption, Eq. (18) captures well the impacts of the pipeline design parameters, operating conditions and the fluid density and expansion coefficient on the line packing times.

4.3. Parametric studies

This section investigates the efficacy of Eq. (18) in describing the effects of operating pressure and temperature on the line packing time for CO_2 transportation pipelines. For this purpose, the line packing time correlation is benchmarked against the results of simulations for hypothetical scenarios of line packing of CO_2 pipelines using the parabolic flow model of Section 2.2, which provides an efficient and robust tool for simulation of pipeline operations involving slow transients.

Simulation of the line packing scenarios using the parabolic model involved calculation of pressure evolution in a pipe, following alteration of the inlet and outlet conditions (in Fig. 1) resulting in imbalanced mass flow into the pipe. Two hypothetical cases are studied: Case A focusing on the impact of initial (operating) pressure, and Case B designed to study the impact of operating temperature on the line packing time. In the case studies, the operating pressures and temperatures were varied in a wide range (pressure from 2 MPa to 12 MPa and temperature between 280 K and 380 K), covering realistic conditions of operation of pipelines transporting both dense phase and gaseous CO_2. The flow rates were chosen from 50 kg s^{-1} to 150 kg s^{-1}, which correspond to typical CO_2 emission rates by large industrial installations. The pipe length, diameter and MAOP were selected to be relevant to, but not necessarily optimal for, the studied operating conditions. In particular, the pipeline diameter was set to 1 m, which is close to optimal size for pipelines transporting the above amounts, while the pipe length was set

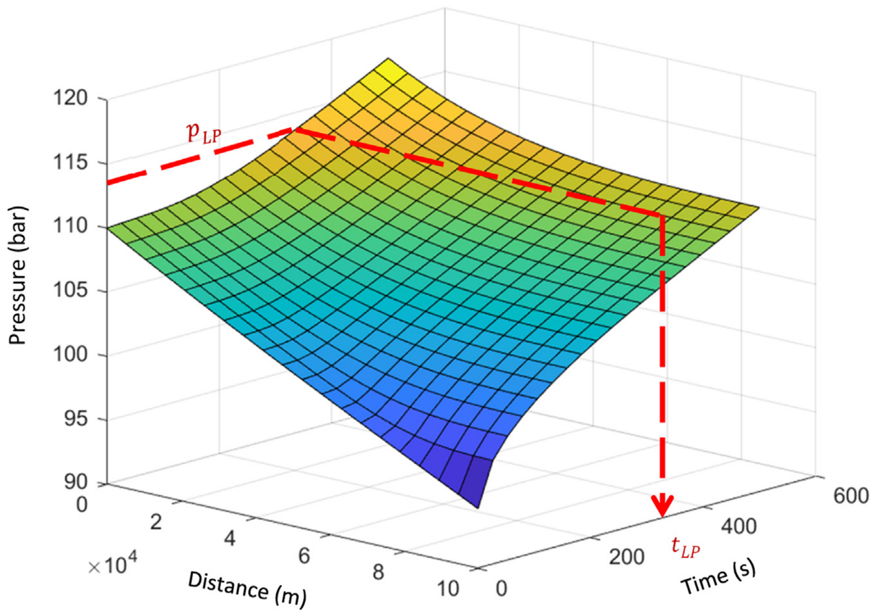

Fig. 3. Illustration of the results of calculation of pipeline pressure variation with time in a line packing scenario where pressure p_{LP} is reached at time t_{LP} (D = 0.44 m, L = 100 km, G_o = 150 kg s^{-1}, T_o = 303 K, $p_{in,o}$ = 11 MPa, p_{LP} = 11.34 MPa).

to 33 km, which approximately corresponds to the largest distance between isolation valves in CO_2 pipelines (IEA GHG, 2003). The MAOP was conservatively estimated at 1 MPa above the pipeline nominal operating pressure.

Assuming the line packing process is isentropic, Eqs. (10) - (13) are solved numerically using the method described in Section 2.3, by advancing the solution in time until the threshold pressure p_{LP} is reached to give the line packing time, t_{LP}, as illustrated in Fig. 3. To achieve the convergence using the spatial discretisation with N_x = 50 points was found to be sufficient.

Case A: The impact of operating pressure

Firstly, a study is performed to investigate the impact of operating pressure on the line packing time. For this purpose, the inlet pressure is varied in the range from 2 to 12 MPa, while the other pipeline design and operation parameters are kept constant, assuming the pipe diameter, D = 1 m, the pipe length L = 33 km, the initial mass flowrate, G_o = 150 kg s^{-1} and the initial temperature, T_o = 303 K. In this case study, the line packing is induced by a 50 % increase in the inlet mass flow rate when the outlet flowrate is unchanged. The line packing pressure threshold p_{LP} is set to 1 MPa above the initial inlet pressure in the pipe, $p_{in,o}$.

Fig. 4 shows that for the studied range of operating pressures, the line packing times estimated using Eq. (18) agree reasonably well with the results obtained from the solution of the parabolic flow model. At low pressures (below ca. 7 MPa at 303 K), which are relevant to gas-phase CO_2 transport, the predicted line packing times are longer than at higher pressures (above ca. 7 MPa at 303 K) relevant for liquid and dense-phase CO_2 transport. This is an expected trend, since gaseous CO_2 has higher compressibility than liquid CO_2. In practical terms, this means that pipelines transporting gas phase CO_2 may offer greater operational flexibility, permitting longer periods (several hours) of temporary increase in the mass flowrate into the pipeline and disruptions at the pipeline discharge end, and hence be better at mitigating fluctuations of CO_2 feed flowrates captured from industrial emitters.

The variation of the line packing time with pressure in Fig. 4 can be explained with the help of Eq. (18), showing that the line packing time decreases with the initial pressure and scales with the ratio ρ/κ_x, i.e. it decreases with the fluid expansion coefficient and increases with the fluid density. In particular, as can be seen in Figure 5(a), at 303 K the ratio ρ/κ_s significantly increases with pressure in the gas phase (pressures

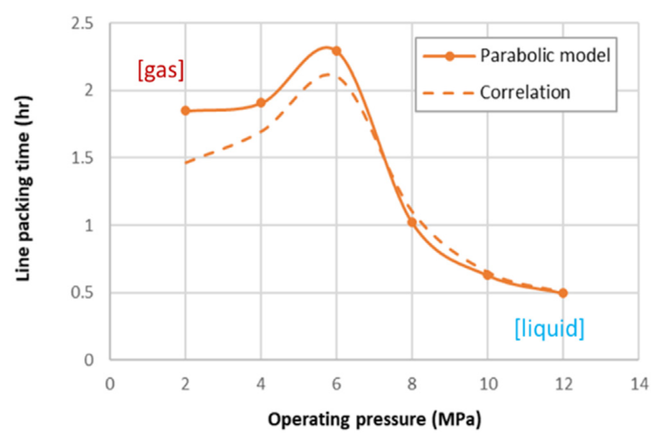

Fig. 4. The line packing times predicted for Case A using the parabolic model and Eq. (18) for different operating pressures (D = 1 m, L = 33 km, $G_{in,o} = G_{out,o} = G_{out}(t>0)$ = 150 kg s^{-1}, $G_{in}(t>0)$ = 225 kg s^{-1}, T_o = 303 K, $p_{LP} = p_{in,o}$ + 1 MPa).

below ca. 7 MPa) – this effect dominates the t_{LP} variation in Fig. 4, and remains nearly constant in the liquid phase (pressures above ca. 7 MPa in Fig. 5) such that t_{LP} in Fig. 4 is mainly affected by the initial operating pressure.

It should be noted that the assumption of isentropic line packing can be justified only for infinitely short line packing times and for well-insulated pipes, so may only work as an approximation for real cases where the pipeline is exchanging heat with the surroundings and the line packing process is not very fast. In the limit of long line packing times and high rates of heat transfer at the pipe wall, the line packing may follow an isothermal path. In Fig. 5a and b, the ratios ρ/κ_s and ρ/κ_t as the key physical properties affecting the line packing time in Eq. (18) are plotted for comparison, showing that isothermal model leads to longer line packing times than in the isentropic model. In practical terms, this means that assuming isentropic line packing gives a conservative estimate of line packing times.

Case B: The impact of operating temperature

In this case, the line packing times are predicted for various initial CO_2 pipeline operating temperatures in a scenario of an outlet isolation

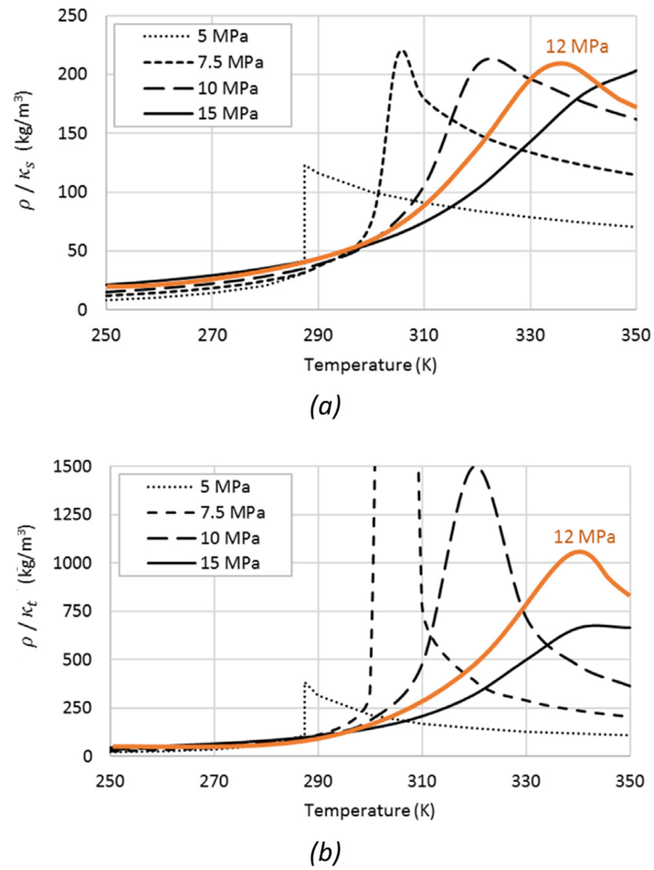

Fig. 5. Variation of the ratios ρ/κ_s (a) and ρ/κ_t (b) for CO_2 with pressure and temperature, as predicted using the Span and Wagner equation of state.

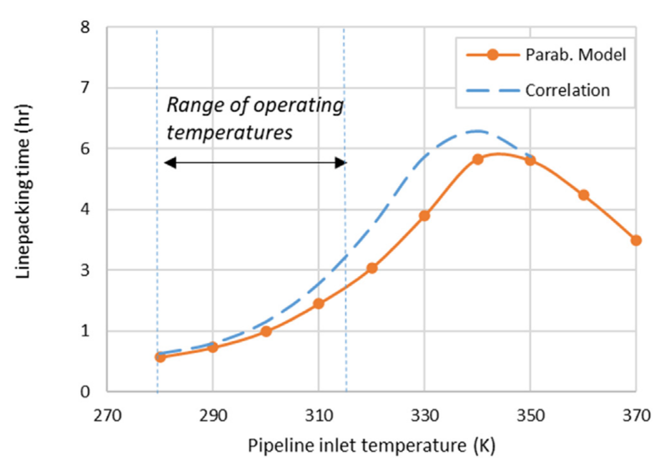

Fig. 6. The line packing times predicted for Case B using the parabolic model and Eq. (18) at different operating pressures.

valve closure, as shown in Fig. 1, i.e. setting G_{out} $(t > 0) = 0$, assuming an initial flowrate of $G_o = 50$ kg s^{-1}. Other design and operating conditions are unchanged (D = 1 m, L = 80 km and $p_{in,o}$ = 12 MPa). Same as in Case A, p_{LP} is set at 1 MPa above $p_{in,\ o}$.

Fig. 6 shows that the line packing times predicted by the parabolic model and Eq. (18) are in good agreement with each other, both varying non-linearly with the pipeline operating temperature. The predicted trend of the line packing time variation with temperature can be easily explained based on Eq. (18), which shows that the line packing times scale with the ρ/κ_s ratio, which also varies with the temperature as shown in Fig. 5. It can be noted that although the line packing time peaks at temperatures in the supercritical phase region (around 345 K), this peak is outside the expected temperature range of CO_2 pipelines operation.

It should be noted that the pressure surge phenomenon induced by instantaneous closure of the outlet valve cannot not be predicted by the parabolic model. This is a result of the simplistic form of the model, which is solely based on the transient continuity equation and cannot describe wave propagation in the pipe, as would be the case when using the full hyperbolic flow model. Practically, in a scenario where the line packing is induced by closure of an isolation valve at the pipe end (Fig. 1), the formation of pressure surge strongly depends on the valve type and its closure rate. The water hammer flow theory predicts that the pressure surge reaches its maximum when the valve closure time is less than the pipeline communication time, $t_{ac} = 2\ L\ /c_s$ (Chaudhry, 1979), while by setting the valve closure duration longer than the pipeline communication time t_{ac}, the pressure surge can be significantly reduced (Yuce and Omer, 2019). In the latter cases, the parabolic flow model and the proposed line packing time correlation can be expected to be accurate approximations of the solution to the hyperbolic flow model (Osiadacz and Gburzyńska, 2022). In other words, at high valve closure rates the pressure surge may happen and this phenomenon cannot be resolved by the parabolic flow model, which predicts the pressure increase only due to the inflow into the pipeline. However, given that the pressure surge lasts only for a short time (commonly associated with t_{ac}), in those cases where the surge magnitude is relatively small compared to the MAOP, the use of the parabolic model and the proposed line packing time correlation can still be justified. As such, predictions based on the parabolic model should always be validated by checking that the pressure surge does not result in pressures exceeding the pipeline MAOP. In the scenarios studied in this section, the pressure surge estimated using the Joukowsky formula, $\Delta p = \rho u c_s$, is less than ca. 70 kPa and 200 kPa for the low-pressure CO_2 transport ($p_{in,o}$ below ca. 5 MPa) and dense-phase CO_2 transport ($p_{in,o}$ up to 12 MPa) respectively, which are significantly smaller than the assumed increase in pressure due to line packing (1 MPa). As such, the use of parabolic model is justified for all the studied cases.

It also should be emphasised that the line packing times calculated in this study were obtained for illustration only and separate calculations should be performed for each specific case and pipeline configuration.

5. Conclusions

Accounting for line packing in the design of pressurised CO_2 transportation pipelines is important to ensure their efficient and safe operation. In particular, line packing time is an important system design parameter affecting the choice of suitable pipeline operational and control strategies, e.g., for maintaining the system pressure below acceptable MAOP threshold in planned operational or accidental scenarios (Giardinella et al., 2022; Peplinski, 2012; Rose, 2015) and smoothing out short-term fluctuations in the feed flowrates to maintain stable downstream conditions for CO_2 utilisation and storage (Mac Dowell and Staffell, 2016; Spitz et al., 2018). To this end, in the present study, a simple algebraic correlation was derived for estimating the line packing time as function of the key design and operation parameters of the pipeline (the pipe volume, nominal operating pressure, mass flowrate and the maximum operating pressure) and physical properties of the fluid (density and expansion coefficient). The correlation was also adopted for the calculation of pipeline unpacking times caused by unbalanced discharge of compressible fluid from a pipeline, which can become practically useful for preventing operability issues that may arise, e.g., due to flashing of liquid CO_2 and transition to two-phase flow when pressure is reduced to below the bubble line pressure (Daud, 2018).

The proposed correlation was shown to deviate by less than 15 % from results of calculations using a transient flow model for dense-phase CO_2 as reported by Aghajani et al. (2017), providing a conservative approximation with the accuracy acceptable for engineering calculations where estimates are usually subject to ca. 10 % variation and uncertainties in the flowrate, pressure and temperature conditions.

The correlation was also verified against predictions of line packing times based on the parabolic flow model simulations for realistic pipelines (up to 80 km long) operating at pressures ranging from 2 to 12 MPa, temperatures from 280 to 330 K and MAOPs of 1 MPa above the nominal operating pressures. The study confirmed that pipelines transporting gas-phase CO_2 offer greater operation flexibility, permitting longer periods (several hours) for mitigation of fluctuations in CO_2 streams due to a temporary increase in the mass flowrate at the pipeline inlet (e.g., due to an increase in CO_2 capture rate from an industrial facility) or reduced flow at the pipeline discharge end (e.g., due to emergency isolation).

The derived line packing time correlation can be practically useful during the conceptual design of pipelines, providing engineers with a rapid method that requires minimal calculations without the recourse to transient flow simulation packages, which become essential for evaluation of line packing scenarios for long pipelines and complex pipeline networks.

It should be noted that the proposed correlation may become inaccurate in those scenarios where physical properties of the fluid, particularly density and compressibility, change significantly during the line packing process. Also, the range of validity of the proposed line packing time correlation is limited to scenarios where line packing is not accompanied by pressure surges, e.g., induced by rapidly closing isolation valves. When this happens, the pressure surge magnitude should be calculated using suitable flow models or correlations.

Declaration of Competing Interest

The authors declare that they have no known competing financial interests or personal relationships that could have appeared to influence the work reported in this paper.

Acknowledgements and disclaimer

This work has received funding from the European Union's Horizon 2020 research and innovation programme under grant agreement no. 884418. The work reflects only the authors' views and the European Union is not liable for any use that may be made of the information contained therein.

Supplementary materials

Supplementary material associated with this article can be found, in the online version, at doi:10.1016/j.ccst.2023.100188.

Appendix

For the numerical solution of the parabolic equations of Section 2.2, they are converted to a PDE in pressure. For this purpose, firstly, the momentum Eq. (9) is differentiated with respect to x:

$$\frac{\partial^2 p}{\partial x^2} = -\frac{f}{2D}\frac{\partial\left(\rho u^2\right)}{\partial x} \tag{21}$$

Using the product rule, the spatial derivative of ρu^2 that appears on the right-hand side of this equation can be expressed as:

$$\frac{\partial\left(\rho u^2\right)}{\partial x} = \rho u\frac{\partial u}{\partial x} + u\frac{\partial(\rho u)}{\partial x} \tag{22}$$

Eliminating in this equation the velocity derivative using the identity $\partial(\rho u) = \rho\,\partial u + u\,\partial\rho$, gives:

$$\frac{\partial\left(\rho u^2\right)}{\partial x} = u\left[\frac{\partial(\rho u)}{\partial x} - u\frac{\partial(\rho)}{\partial x}\right] + u\frac{\partial(\rho u)}{\partial x} \tag{23}$$

Substituting Eq. (23) into Eq. (21) and then using the continuity Eq. (8) to eliminate the partial derivative $\frac{\partial(\rho u)}{\partial x}$, results in:

$$\frac{\partial^2 p}{\partial x^2} = -\frac{f}{2D}\left[-2u\frac{\partial\rho}{\partial t} - u^2\frac{\partial\rho}{\partial x}\right] \tag{24}$$

Using the density-pressure relation defined by the process-specific (e.g., isentropic or isothermal) speed of sound:

$$c_z = \sqrt{\left(\frac{\partial p}{\partial\rho}\right)_z} \tag{25}$$

the density derivatives in equation (24) can be changed to derivatives of pressure:

$$\frac{\partial^2 p}{\partial x^2} = \frac{f}{2Dc_z^2}\left[2u\frac{\partial p}{\partial t} + u^2\frac{\partial p}{\partial x}\right] \tag{26}$$

Expressing in this equation the velocity u in terms of the pressure gradient according to the momentum Eq. (9), results in the final form of the PDE for pressure:

$$\frac{1}{c_z^2}\sqrt{\frac{2}{\rho}\frac{f}{D}\left|\frac{\partial p}{\partial x}\right|}\frac{\partial p}{\partial t} - \frac{1}{\rho c_z^2}\left(\frac{\partial p}{\partial x}\right)^2 - \frac{\partial^2 p}{\partial x^2} = 0 \tag{27}$$

References

Abbaspour, M., Krishnaswami, P., Chapman, K.S., 2007. Transient optimization in natural gas compressor stations for linepack operation. J. Energy Resour. Technol. 129 (4), 314–324. doi:10.1115/1.2790983, Transactions of the ASME.
Aghajani, H., Race, J.M., Wetenhall, B., Sanchez Fernandez, E., Lucquiaud, M., Chalmers, H., 2017. On the potential for interim storage in dense phase CO_2 pipelines. Int. J. Greenhouse Gas Control 66 (December 2016), 276–287. doi:10.1016/j.ijggc.2017.06.002.
Ahmadian Behrooz, H., Boozarjomehry, R.B., 2017. Dynamic optimization of natural gas networks under customer demand uncertainties. Energy 134, 968–983. doi:10.1016/j.energy.2017.06.087.
Aursand, P., Hammer, M., Munkejord, S.T., Wilhelmsen, O., 2013. Pipeline transport of CO_2 mixtures: models for transient simulation. Int. J. Greenhouse Gas Control 15, 174–185. doi:10.1016/j.ijggc.2013.02.012.
binti Daud, N.K., 2018. Multistage compression and transient flow in CO_2 pipelines with line packing. PhD Thesis. University College London.
Chaudhry, M.H., 1979. Applied Hydraulic Transients. VNR.
Chertkov, M., Backhaus, S., Lebedev, V., 2015. Cascading of fluctuations in interdependent energy infrastructures: gas-grid coupling. Appl. Energy 160, 541–551. doi:10.1016/j.apenergy.2015.09.085.
Doctor, R., Palmer, A., Coleman, D., Davison, J., Hendriks, C., Kaarstad, O., & Ozaki, M. (2005). Transport of CO_2. In IPCC Special Report on Carbon Dioxide Capture and Storage.
IEA GHG, 2003. Barriers to Overcome in Implementation of CO_2 Capture and Storage (2): Rules and Standards for the Transmission and Storage of CO_2. IEA Greenhouse Gas R & D Programme Report PH4/23.
Ejeh, J.O., Yousef, A.Z., Bugryniec, P.J., Wilkes, M.D., Porter, R.T.J., Martynov, S.B., Mahgerefteh, H., Brown, S.F., 2022. Perspectives on future CCUS infrastructure design. In: Proceedings of the 16th International Conference on Greenhouse Gas Control Technologies, GHGT-16 23rd.
Giardinella, S., Obrien, K.C., Gioja, L., Dexter, J., Baumeister, A., Roberts, D., Callahan, R., Roman, R.R., Prausse, S., Larimore, R., Baroi, C., 2022. Compressed CO_2 energy storage on CO_2 transport pipelines. SSRN Electronic J. 1–11 October.
Lemmon, E.W., Bell, I.H., Huber, M.L., McLinden, M.O., 2018. REFPROP Documentation, Release 10.0. NIST, p. 135 June 04, 2018.
Mac Dowell, N., Staffell, I, 2016. The role of flexible CCS in the UK's future energy system. Int. J. Greenhouse Gas Control 48, 1–18. doi:10.1016/j.ijggc.2016.01.043.
Martynov, S., Mac Dowell, N., Brown, S., Mahgerefteh, H., 2015. Assessment of integral thermo-hydraulic models for pipeline transportation of dense-phase and supercritical CO_2. Ind. Eng. Chem. Res. 54 (34), 8587–8599. doi:10.1021/acs.iecr.5b00851.
MathWorks. (2023). PDEPE function. In MatLab Documentation. https://uk.mathworks.com/help/matlab/ref/pdepe.html
Oosterkamp, A., Ramsen, J., 2008. State-of-the-Art Overview of CO_2 Pipeline Transport with relevance to offshore pipelines. Report to the Research Council of Norway Report Number POL-O-2007-138-A.
Osiadacz, A., 1984. Simulation of transient gas flows in networks. Int. J. of Num. Methods Fluids 4, 13–24. doi:10.1002/fld.165004010.
Osiadacz, A.J., Gburzyńska, M., 2022. Selected mathematical models describing flow in gas pipelines. Energies 15 (478), 1–20. doi:10.3390/en15020478.
Pambour, K.A., Bolado-Lavin, R., Dijkema, G.P.J., 2016. An integrated transient model for simulating the operation of natural gas transport systems. J. Nat. Gas Sci. Eng. 28, 672–690. doi:10.1016/j.jngse.2015.11.036.
Pambour, K.A., Erdener, B.C., Bolado-Lavin, R., Dijkema, G.P.J., 2017. Development of a simulation framework for analyzing security of supply in integrated gas and electric power systems. Appl. Sci. 7 (1). doi:10.3390/app7010047.

Peplinski, S. (2012). Basic Design & Engineering Package. Quest CCS Project Report 07-1-AA-7739-0001.
Rackley, S.A., 2010. Carbon dioxide transportation. Carbon Capture Storage 329–344. doi:10.1016/b978-1-85617-636-1.00015-8.
Ríos-Mercado, R.Z., Borraz-Sánchez, C., 2015. Optimization problems in natural gas transportation systems: a state-of-the-art review. Appl. Energy 147, 536–555. doi:10.1016/j.apenergy.2015.03.017.
Shashi Menon, E. (2005). Gas Pipeline Hydraulics. https://doi.org/10.1201/9781420038224
Skeel, R.D., Berzins, M., 1990. A method for the spatial discretization of parabolic equations in one space variable. SIAM J. Sci. Stat. Comput. 11 (1), 1–32. doi:10.1137/0911001.
Span, R., Wagner, W., 1996. A new equation of state for carbon dioxide covering the fluid region from the triple point temperature to 1100K at pressures up to 800MPa. J. Phys. Chem. B 25, 1509–1596.
Spitz, T., Avagyan, V., Ascui, F., Bruce, A.R.W., Chalmers, H., Lucquiaud, M., 2018. On the variability of CO_2 feed flows into CCS transportation and storage networks. Int. J. Greenhouse Gas Control 74 (May), 296–311. doi:10.1016/j.ijggc.2018.04.008.
White Rose. (2015). K34 : Flow Assurance. Technical Report (Issue November).
Yuce, M.I., Omer, A.F., 2019. Hydraulic transients in pipelines due to various valve closure schemes. SN Appl. Sci. (9) 1. doi:10.1007/s42452-019-1146-4.
ZEP. A Trans-European CO_2 Transportation Infrastructure for CCUS: Opportunities & Challenges.